

# Field-induced superdiffusion and dynamical heterogeneity

Giacomo Gradenigo,<sup>1</sup> Eric Bertin,<sup>1</sup> and Giulio Biroli<sup>2</sup>

<sup>1</sup> *Université Grenoble Alpes, LIPHY, F-38000 Grenoble, France*

*CNRS, LIPHY, F-38000 Grenoble, France*

<sup>2</sup> *IPhT, Université Paris Saclay, CEA, CNRS, F-91191 Gif-sur-Yvette Cedex, France*

*Laboratoire de Physique Statistique, Ecole Normale Supérieure,*

*PSL Research University; Université Paris Diderot Sorbonne Paris-Cité; Sorbonne*

*Universités UPMC Univ. Paris 06; CNRS; 24 rue Lhomond, 75005 Paris, France.*

(Dated: April 12, 2016)

By analyzing two Kinetically Constrained Models of supercooled liquids we show that the anomalous transport of a driven tracer observed in supercooled liquids is another facet of the phenomenon of dynamical heterogeneity. We focus on the Fredrickson-Andersen and the Bertin-Bouchaud-Lequeux models. By numerical simulations and analytical arguments we demonstrate that the violation of the Stokes-Einstein relation and the observed field-induced superdiffusion have the same physical origin: while a fraction of probes do not move, others jump repeatedly because they are close to local mobile regions. The anomalous fluctuations observed out of equilibrium in presence of a pulling force  $\epsilon$ ,  $\sigma_x^2(t) = \langle x_\epsilon^2(t) \rangle - \langle x_\epsilon(t) \rangle^2 \sim t^{3/2}$ , which are accompanied by the asymptotic decay  $\alpha_\epsilon(t) \sim t^{-1/2}$  of the non-Gaussian parameter from non-trivial values to zero, are due to the splitting of the probes population in the two (mobile and immobile) groups and to dynamical correlations, a mechanism expected to happen generically in supercooled liquids.

Superdiffusion in presence of an external driving is one among the most intriguing results of microrheological numerical experiments in supercooled liquid [1, 2] and of experimental studies on glassy granular media [3]. In supercooled liquids the mean square displacement (MSD) of a tagged particle displays a characteristic intermediate plateau of increasing length when the temperature is lowered, due to caging, while asymptotically the diffusion is always Fickian,  $\langle x^2(t) \rangle \sim t$ . The surprising finding of [1, 2] is that, notwithstanding the slowing down of the dynamics, at low enough temperatures the action of an external force on a probe particle produces a superdiffusive spreading of the probability distribution of displacements, namely  $\sigma_x^2(t) = \langle x_\epsilon^2(t) \rangle - \langle x_\epsilon(t) \rangle^2 \sim t^\gamma$  with  $\gamma > 1$  and with  $\epsilon$  representing a force acting on the probe. This *anomalous* behaviour of the mean square displacement (MSD) around the drift is really a landmark of non-Fickian diffusion: in the case of Fickian diffusion the MSD around the drift would grow linearly in time,  $\sigma_x^2(t) \sim t$ , as the unbiased MSD does. What is the mechanism which triggers a faster-than-Fickian diffusion within an environment with large and broadly distributed relaxation times? At first sight this is a quite counter-intuitive behaviour. The goal of this paper is to provide a clear-cut explanation of such a mechanism, clarifying how this anomalous diffusion is intimately related to dynamical heterogeneities and to the breaking of the Stokes-Einstein relation.

The Stokes-Einstein (S-E) relation connects the diffusion coefficient  $D(\beta)$  of a probe to the relaxation time  $\tau_{\text{eq}}(\beta)$  of the sample as  $D(\beta)\tau_{\text{eq}}(\beta) = \text{const}$  [4]. The physical reason for such relation is that simple liquids are characterized by a single relevant time-scale  $\tau_D$ : this time-scale characterizes the behaviour of the system at all scales, from the single molecule diffusion,  $D(\beta) \sim \tau_D^{-1}(\beta)$ , to

the relaxation of the sample  $\tau_{\text{eq}}(\beta) \sim \tau_D(\beta)$ , which explains the Stokes-Einstein relation. Close to the glass-transition temperature  $T_g$  several time-scales appear in the dynamics of the system. In this regime the characteristic diffusion time  $\tau_D(\beta) \sim D^{-1}(\beta)$  *decouples* from the relaxational time,  $\tau_{\text{eq}}(\beta) \approx \tau_D(\beta)$ , so that one also finds  $D(\beta)\tau_{\text{eq}}(\beta) \neq \text{const}$  [5]: this is the Stokes-Einstein violation. A particularly instructive and useful rationalization of this phenomenon was obtained studying Kinetically Constrained Models (KCM) [6–14]. These are lattice models where a mobility field with local update rules subjected to kinetic constraints reproduces the sluggish and heterogeneous dynamics of glasses. The heterogeneous nature of space-time correlations is explained in KCMs in terms of *defects* dynamics. The activity field of KCMs is characterized by rare *mobility* defects which, wandering around in the system, trigger the relaxation of the whole sample. We show here that this very same mechanism also leads to the anomalous transport properties observed in [1, 2]. Looking at the motion of a driven intruder, the heterogeneous nature of the medium becomes manifest only in the *out-of-equilibrium* fluctuations  $\sigma_x^2(t)$ : this is the case also for the diffusion on hierarchical lattices discussed in [15], and for the field-induced superdiffusion of tracer in a crowded medium discussed in [16].

We study the driven dynamics of a tracer particle in two kinetically constrained models: the one-dimensional Fredrickson-Andersen (FA) [6–8] and Bertin-Bouchaud-Lequeux (BBL) models [9, 12]. Both have been studied and used as models of supercooled liquids. The local structure in FA is described by a binary variable  $n_i \in \{0, 1\}$ : sites with  $n_i = 1$  are active while those with  $n_i = 0$  are inactive. The update of  $n_i$  is possible only when at least one among its neighbours is already

active, namely one needs  $n_{i+1} = 1$  or  $n_{i-1} = 1$ . When possible, the update  $1 \rightarrow 0$  is always accepted, while  $0 \rightarrow 1$  takes place with probability  $e^{-\beta}$ , where  $\beta$  is a dimensionless inverse temperature. The dynamics obeys detailed balance, with an energy function  $E = \sum_i n_i$ , so that the equilibrium state has no correlations between sites. The FA model exhibits non-trivial correlated dynamics for  $\beta \gtrsim 1$ . The concentration of active sites is  $c = \langle n_i \rangle = [1 + e^\beta]^{-1}$ . Lengths are in units of the lattice spacing which we set to one. The BBL model is described by a continuous variable: the density of mass  $\rho_i \in [0, \infty)$ . The elementary step of the BBL dynamics is the simultaneous update of the density in a couple of neighbouring sites  $\rho_i$  and  $\rho_j$ :  $\rho'_i = q(\rho_i + \rho_j)$  and  $\rho'_j = (1 - q)(\rho_i + \rho_j)$ , with  $q \in [0, 1]$ . The update is possible only when the densities of the two sites fulfill the constraint  $(\rho_i + \rho_j)/2 < \rho_{th} = 1$ : the BBL is a kinetically constrained mass transport model. The random variable  $q$ , which introduces stochasticity in the dynamics of the density field, is extracted from a distribution  $\psi_\mu(q)$  characterized by the parameter  $\mu$ . In the present study we consider the value  $\mu = 0.3$ , which produces a diffusive dynamics of the mobility defects, which are represented by the *active* links where the kinetic constraint is fulfilled. Details on the dynamics of the mobility defects for different values of  $\mu$  can be found in [9, 12]. In the BBL model the definition of *active* links is naturally encapsulated into the definition of the model. In the FA model a link between two sites  $i$  and  $i + 1$  is *active* when both are active,  $n_i = n_{i+1} = 1$ .

Following [10, 11] we model micro-rheological experiments by assuming that the driven tracer can only move between two adjacent sites when these form an active link. Since the updates of  $n_i$  in FA and of the mass field  $\rho_i$  in BBL do not depend on the position of the probe the latter behaves as a *ghost* particle: it is influenced by the background but has no influence on it. In order to induce a directed motion of the probe we unbalance in both models the probability of its forward and backward displacements:  $p_\epsilon^+ = 1/2 + \epsilon$ ,  $p_\epsilon^- = 1/2 - \epsilon$ , with  $\epsilon \in [-1/2, 1/2]$ . The dynamics of a ghost probe in both the FA and the BBL can be then fully understood in terms of the mobility defects dynamics [7, 10]. The dynamics of the probe is ruled by two relevant time-scales: the mean *persistence* time, which is the time the probe has to wait on average before being hit for the first time by a defect, and the average *exchange* time, which is the time between two successive meetings with a defect. The difference between these two time-scales is both the signature of heterogeneous dynamics and the key ingredient of the anomalous transport of a probe. There is only one difference for the defects dynamics of the two models: while in the BBL the diffusion coefficient of defects does not depend on their concentration  $c$ , in the FA model the diffusion of mobile defects depends on the temperature, and hence on their concentration. Henceforth, in order

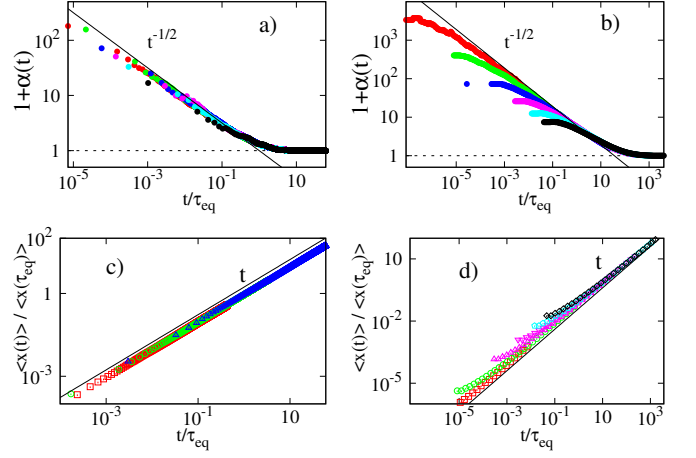


FIG. 1. *Panels a), b)*: Data collapse for the non-Gaussian parameter  $\alpha_\epsilon(t)$  obtained plotting  $1 + \alpha_\epsilon(t)$  vs  $t/\tau_{eq}$  for the different concentrations of mobility defects (different symbols) in FA [a)] and BBL [b)]. The continuous straight line emphasizes the behaviour  $\alpha_\epsilon(t) \sim t^{-1/2}$  in the pre-asymptotic regime. The different concentrations of mobility defects are:  $c = 10^{-2}, 6.7 \cdot 10^{-3}, 5.2 \cdot 10^{-3}, 3.8 \cdot 10^{-3}, 2.8 \cdot 10^{-3}, 1.9 \cdot 10^{-3}$  for the FA model;  $c = 2 \cdot 10^{-1}, 1.1 \cdot 10^{-1}, 5.1 \cdot 10^{-2}, 1.6 \cdot 10^{-2}, 2.7 \cdot 10^{-3}, 2.8 \cdot 10^{-4}$  for the BBL model. *Panels c), d)*: Drift of the probe in FA [c)] and BBL [d)]; data are at the same concentrations of mobility defects of panels a) and b). Collapse is obtained plotting  $\langle x_\epsilon(t) \rangle / \langle x_\epsilon(\tau_{eq}) \rangle$  vs  $t/\tau_{eq}$ .

to present a unified discussion for the two models, time is measured in the units of  $\tau_0$ , which is the time-scale on which a mobile defect moves of one step ( $1/c$  and 1 for the FA and the BBL models respectively).

Assuming that defects are independent random walkers the dynamics of the probe can be described as a Continuous Time Random Walk (CTRW) [10]. In this approximation the histogram of probe displacements, which corresponds to the self part of the van Hove function  $G_s(r, t) = \langle \delta(r - [x(t) - x(0)]) \rangle$  (the angular brackets indicate the average over different trajectories), can be exactly written with the following formula [10]:

$$G_s(x, t) = \mathcal{P}(t)\delta(x) + \int_0^t p(t-s)P_{1st}(x, s) ds. \quad (1)$$

In Eq. (1) the probability of persistence times is denoted by  $p(t-s)$ ,  $P_{1st}(x, s)$  is the propagator for trajectories which start with a jump event (the subscript <sub>1st</sub> indicates that at least one displacement took place) and  $\mathcal{P}(t)$  is the persistence function, i.e., the probability that a probe is not hit by a mobility defect for a duration of  $t$  when the observation starts at an arbitrary time. From Eq. (1) is clear that the population (or the probability) is split into two groups: probes which at time  $t$  have already started to move and probes which at  $t$  are still at rest (we refer to a population of probes since we can think of having many probes evolving in parallel and starting from random positions). Since in both FA and BBL

models defects behave as independent random walkers, persistence equals the survival probability  $\mathcal{P}(t) = e^{-c\sqrt{t}}$ , with  $c$  the concentration of walkers [17]. The distribution of persistence times  $p(t)$  which enters Eq. (1), and is obtained as  $p(t) = -d\mathcal{P}(t)/dt = c e^{-c\sqrt{t}}/\sqrt{t}$ . The distribution of exchange times, which is in turn proportional to  $-dp(t)/dt$  [11], reads to leading order in  $c$  as  $\psi(\tau) = c e^{-c\sqrt{\tau}}/\tau^{3/2}$ . The representation of the probe dynamics as a CTRW is very insightful and will be our main tool to understand the relationship between dynamic heterogeneity and anomalous diffusion of a driven tracer.

We now present our numerical results about anomalous diffusion in the FA and BBL models, which are shown in Fig. 1 and Fig. 2. By looking at Fig. 1 we notice that a driven probe ( $\epsilon = 1/2$ ) has a linear drift in both FA and BBL, but at the same time the non-Gaussian parameter  $\alpha_\epsilon(t)$  for non-centered distributions signals important deviations from Gaussianity up to  $t \sim \tau_{\text{eq}}$ . For a Gaussian distribution with mean  $\langle x_\epsilon(t) \rangle$  and variance  $\sigma_x(t)$  the fourth non-centered moment reads  $\langle x_\epsilon^4(t) \rangle = \langle x_\epsilon(t) \rangle^4 + 6\langle x_\epsilon(t) \rangle^2 \sigma_x^2(t) + 3\sigma_x^4(t)$ , which allows us to define  $\alpha_\epsilon(t)$  as:

$$\alpha_\epsilon(t) = \frac{\langle x_\epsilon(t)^4 \rangle}{\langle x_\epsilon(t) \rangle^4 + 6\langle x_\epsilon(t) \rangle^2 \sigma_x^2(t) + 3\sigma_x^4(t)} - 1, \quad (2)$$

where  $\sigma_x^2(t) = \langle x_\epsilon^2(t) \rangle - \langle x_\epsilon(t) \rangle^2$ . It can be easily seen that with zero drift the standard definition of the non-Gaussian parameter is recovered. For aesthetic reasons in Fig. 1 we plotted  $1 + \alpha_\epsilon(t)$ . Eq. (1) tells us that the overall drift comes from the convolution of the drift of the moving probes with the distribution of persistence times:

$$\langle x_\epsilon(t) \rangle = \int_0^t ds p(t-s) \langle x_\epsilon(s) \rangle_{1\text{st}}. \quad (3)$$

From the inspection of Eq. (3) is possible to single out the different physical mechanisms [18] which determine the linear behaviour of the drift,  $\langle x_\epsilon(t) \rangle \sim t$ , in the two regimes  $1 \ll t \ll \tau_{\text{eq}}$  and  $\tau_{\text{eq}} \ll t$ . In the latter, due to the exponential cut-off of  $\psi(\tau)$ , for  $t \gg \tau_{\text{eq}} = c^{-2}$  the drift  $\langle x_\epsilon(s) \rangle_{1\text{st}}$  is linear. In this regime one can approximate  $\int_0^t ds p(t-s) \langle x_\epsilon(s) \rangle_{1\text{st}} \sim (1 - \mathcal{P}(t)) \langle x_\epsilon(t) \rangle_{1\text{st}} \sim \langle x_\epsilon(t) \rangle_{1\text{st}}$ , which shows that the total drift is also linear. On the contrary, in the former regime that we will call pre-asymptotic henceforth, persistence and exchange distributions can be approximated by power-law distributions:  $\psi(\tau) \sim \tau^{-3/2}$  and  $p(t) \sim t^{-1/2}$ . This leads to a subdiffusion of the moving probe as  $\langle x_\epsilon(t) \rangle_{1\text{st}} \sim \sqrt{t}$ . The physical reason is that moving probes are repeatedly hit by a mobile defect  $t^{1/2}$  times. On the other hand the fraction of moving probes increases too, as  $c\sqrt{t}$ , due to the heavy tail of  $p(t)$ . How these two effects combine can be read off in the explicit expression of Eq. (3) in the regime  $t \ll \tau_{\text{eq}}$ , i.e.,  $\langle x_\epsilon(s) \rangle \sim c \int_0^t ds (t-s)^{-1/2} \sqrt{s}$ :

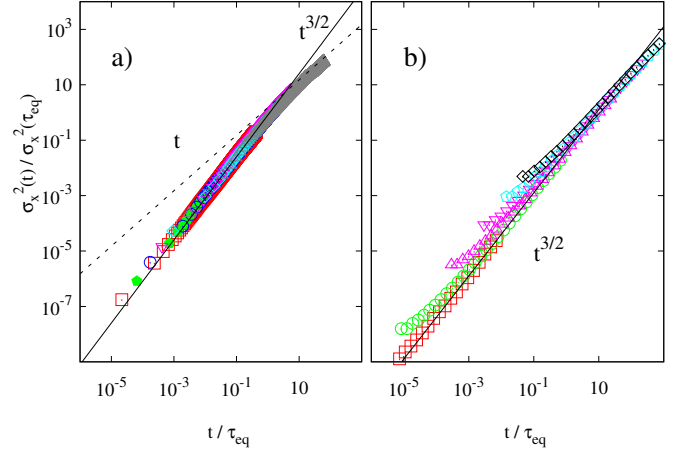


FIG. 2. Mean square displacement around the drift  $\sigma_x^2(t)$  for a driven probe ( $\epsilon = 1/2$ ) in FA [panel a)] and BBL [panel b)]. Different symbols represent different concentrations  $c$  of the mobility defects, which are, respectively for the two models, the same as in Fig. 1. Collapse of the curves is obtained by plotting  $\sigma_x^2(t)/\sigma_x^2(\tau_{\text{eq}})$  vs  $t/\tau_{\text{eq}}$ . Full line is the  $t^{3/2}$  scaling, dashed line [only panel a), FA] is the Fickian behaviour  $\sigma_x^2(t) \sim t$ .

the change of variable  $s \rightarrow s/t$  in the last integral yields immediately  $\langle x_\epsilon(s) \rangle \sim c t$ . It is due to this non-trivial mechanism that, even in the pre-asymptotic regime, we can observe a linear drift.

Fig. 2 shows then that the non-Gaussianity of  $G_\epsilon(x, t)$  is manifest in the transport properties of the intruder when one looks at the MSD around the drift  $\sigma_x^2(t) = \langle x_\epsilon^2(t) \rangle - \langle x_\epsilon(t) \rangle^2$ : it grows superdiffusively as  $\sigma_x^2(t) \sim t^\gamma$  with  $\gamma \approx 3/2$  for  $1 \ll t \ll \tau_{\text{eq}}$ . The exponent  $3/2$  is the same which characterizes the field-induced superdiffusion of a tracer in a crowded medium [16]. The population splitting scenario, recently discussed also in the context of CTRW with aging dynamics [20, 21], allows one to perfectly understand both qualitatively and quantitatively not only the observed superdiffusion (Fig. 2), but also the pre-asymptotic behaviour of the non-Gaussian factor (Fig. 1).

From the definition of  $G_s(x, t)$  in Eq. (1) we have that the MSD around the drift reads

$$\sigma_x^2(t) = -\langle x_\epsilon(t) \rangle^2 + \int_0^t ds p(t-s) \langle x_\epsilon^2(s) \rangle_{1\text{st}}. \quad (4)$$

We already know that in the pre-asymptotic regime  $\langle x_\epsilon(t) \rangle \sim c t$ , so that we only need to know  $\langle x_\epsilon^2(s) \rangle_{1\text{st}}$ . The latter is obtained from the asymptotic behaviour of moments for a biased CTRW [19, 22–24]. In a CTRW with waiting time distribution  $\psi(\tau) \sim \tau^{-(1+\beta)}$  and  $0 < \beta < 1$  it holds  $\langle x_\epsilon^2(t) \rangle \sim t^{2\beta}$ : since in our case  $\beta = 1/2$ , we have  $\langle x_\epsilon^2(s) \rangle_{1\text{st}} \sim s$ . By plugging this last result in Eq. (4) and retaining the leading contribution to  $p(t-s)$

when  $t \ll \tau_{\text{eq}}$ , one finds

$$\sigma_x^2(t) \sim c \int_0^t ds \frac{s}{\sqrt{t-s}} \sim c t^{3/2}, \quad (5)$$

where the asymptotic behaviour of the integral has been evaluated by simply changing variable  $s \rightarrow s/t$ . The term  $\langle x_\epsilon(t) \rangle^2 = O(c^2)$  appearing in Eq. (4) has been dropped in Eq. (5) because it is subleading in the regime  $c \ll 1$ ,  $t \ll \tau_{\text{eq}}$ . We obtained analytically the superdiffusive behaviour tracing it back to the subsequent hits with the mobile defects, which are in turn encoded in the heavy tails of  $\psi(\tau)$ . To estimate the pre-asymptotic behaviour of the non-Gaussian parameter  $\alpha_\epsilon(t)$  we need to know the fourth order non-centered moment, which from Eq. (1) reads:

$$\langle x_\epsilon^4(t) \rangle = \int_0^t ds \frac{c}{\sqrt{t-s}} \langle x_\epsilon^4(s) \rangle_{1\text{st}} \sim c t^{5/2}. \quad (6)$$

The scaling in Eq. (6) comes again from the asymptotic behaviour of moments in a CTRW characterized by the distribution of waiting times  $\psi(\tau) \sim \tau^{-(1+\beta)}$  and  $0 < \beta < 1$ :  $\langle x_\epsilon^4(s) \rangle \sim s^{4\beta}$  [22, 23]. Since in our case  $\beta = 1/2$  we have  $\langle x_\epsilon^4(s) \rangle \sim s^2$ . For small values of  $c$  the denominator of the non-Gaussian parameter reads at leading order:

$$\langle x_\epsilon(t) \rangle^4 + 6 \langle x_\epsilon(t) \rangle^2 \sigma_x^2(t) + 3 \sigma_x^4(t) \sim 3 c^2 t^3, \quad (7)$$

so that, combining Eq. (6) with Eq. (7) we find:

$$\alpha_\epsilon(t) \sim c^{-1} t^{-1/2}, \quad (8)$$

which is perfectly consistent with the numerical behaviour of  $\alpha_\epsilon(t)$  shown in Fig. 1. *Strong* anomalous diffusion takes place when the scaling assumption  $G_s(x, t) = \mathcal{F}[x/\ell(t)]/\ell(t)$  for the van Hove function and the scaling of moments,  $\langle x^n(t) \rangle \sim \ell^n(t)$ , *cannot* be written in terms of a single length  $\ell(t)$  [19]. In the present case (FA and BBL) this phenomenon takes place due to population splitting. Looking at the distribution of moving probes we have found the numerical evidence (not shown) that  $P_{1\text{st}}(x_\epsilon, t)$  is a half-Gaussian: at different times a perfect collapse of data is obtained with  $\ell(t) = t^{1/2}$ . Taking otherwise into account the whole population of probes, i.e. also the contribution  $\mathcal{P}(t)\delta(x)$ , in Eq.(1), of probes which never jumped up to time  $t$ , we have  $\sigma_x^2(t) \sim t^{3/2} \neq \ell^2(t) = t$ : diffusion is *strongly* anomalous [19]. Let us stress that this strong anomalous diffusion is not due, as usual, to a multiscaling property of the probability distribution of displacements [19]: it comes from the splitting of probes population into slow persistent ones, not moving roughly until  $t \sim \tau_{\text{eq}}$ , and those which already at  $t \ll \tau_{\text{eq}}$  have already been repeatedly hit by mobility defects. Precisely the same mechanisms is at the origin of S-E violation  $D \tau_{\text{eq}} = e^{-\beta}$ : a probe diffuses much more than one step

on the relaxation time-scale due to repeated interactions with the same mobile defect. Such a mechanism is also responsible for dynamic heterogeneity: all regions that relax because they are hit by the same mobile defect within the time-scale  $\tau_{\text{eq}}$  become dynamically correlated. We have therefore shown that dynamic correlations, violation of S-E and *strong* anomalous superdiffusion are directly connected in KCMs [10] (see also [14]).

In conclusion we have related the superdiffusive behaviour of driven probes to the splitting of their population in frozen ones and moving ones repeatedly hit by the same mobility defect. Our analysis provides an explanation of the results found in atomistic models [1, 2] and link them to the phenomena of dynamic heterogeneity and Stokes-Einstein violation. Furthermore, it offers a theoretical derivation of the superdiffusion exponent  $3/2$ . This value, compatible with our numerical results for both the FA and the BBL model, is also surprisingly close to the value 1.45 found in the supercooled Yukawa mixture of [2]. It is also remarkable the qualitative agreement between the behaviour of the non-Gaussian factor  $\alpha_\epsilon(t)$  characterizing the driven pre-asymptotic dynamics of a probe in one-dimensional FA and BBL models and the one found for the unbiased dynamics of a probe in a three-dimensional supercooled Lennard-Jones mixture (see Fig. 3 of [1]). All these similarities point towards the presence of universal features, still to be investigated, which are intrinsically related to dynamical heterogeneity and emerge at low temperatures independently from the dimensionality and the specific interactions of the models. We expect indeed our findings to hold generically beyond the simple models we focused on. In fact, the key ingredients are the population splitting scenario and the anomalous diffusion of mobile probes induced by dynamic correlations, which are phenomena known to be present generically in supercooled liquids.

G.G. acknowledges support from the ERC Grant GLASSDEF No. ADG20110209. G.B. acknowledges support from the ERC Grant NPRGGLASS. We wish to thank E. Barkai, J.-L. Barrat, O. Bénichou and A. Heuer for useful discussions and comments.

- 
- [1] C. F. E. Schroer and A. Heuer, Phys. Rev. Lett. **110**, 067801 (2013).
  - [2] D. Winter, J. Horbach, P. Virnau and K. Binder, Phys. Rev. Lett. **108** 028303 (2012).
  - [3] F. Lechenault, R. Candelier, O. Dauchot, J.P. Bouchaud, G. Biroli, Soft Matter **6**, 3059 - 3064, 2010.
  - [4] One can consider all the extra factors as constant since their variation is very slow.
  - [5] G. Tarjus, D. Kivelson, J. Chem. Phys **103** 3071 (1995).
  - [6] G. H. Fredrickson and H. C. Andersen, Phys. Rev. Lett **53**, 1244 (1984).

- [7] J. P. Garrahan and D. Chandler, Phys. Rev. Lett. **89**, 035704 (2002).
- [8] L. Berthier and J.P. Garrahan, Phys. Rev. E **68**, 041201 (2003).
- [9] E. Bertin, J.-P. Bouchaud, F. Lequeux **95**, 015702 (2005).
- [10] L. Berthier, D. Chandler, J.-P. Garrahan, Europhys. Lett. **69** (3), 320-326 (2005).
- [11] Y. Jung, J.-P. Garrahan, D. Chandler, J. Chem. Phys. **123**, 084509 (2005).
- [12] R.-L. Jack, P. Sollich, P. Meyer, Phys. Rev. E **78**, 061107 (2008).
- [13] R.-L. Jack, D. Kelsey, J. P. Garrahan, and D. Chandler, Phys. Rev. E **78**, 011506 (2008).
- [14] O. Blondel, C. Toninelli, EPL **107** 26005 (2014).
- [15] G. Forte, F. Cecconi, A. Vulpiani, Eur. Phys. J. B **87**, 102 (2014).
- [16] O. Bénichou, A. Bodrova, D. Chakraborty, P. Illien, A. Law, C. Mejía-Monasterio, G. Oshanin, and R. Voituriez, Phys. Rev. Lett. **111**, 260601 (2013).
- [17] S. Redner, *A guide to First-Passage Processes*, Cambridge University Press, Cambridge, England (2001).
- [18] P. Illien, O. Bénichou, G. Oshanin, and R. Voituriez, Phys. Rev. Lett. **113**, 030603 (2014).
- [19] P. Castiglione, A. Mazzino, P. Muratore-Ginanneschi, and A. Vulpiani, Physica D **134**, 75 (1999).
- [20] J. Schulz, E. Barkai, R. Metzler Phys. Rev. Lett. **110**, 020602 (2013).
- [21] J. Schultz, E. Barkai, R. Metzler Physical Review X, **4**, 011028 (2014)
- [22] R. Burioni, G. Gradenigo, A. Sarracino, A. Vezzani, A. Vulpiani, J. Stat. Mech. P09022 (2013).
- [23] R. Burioni, G. Gradenigo, A. Sarracino, A. Vezzani, A. Vulpiani, Commun. Theor. Phys. **62**, 514 (2014).
- [24] G. Gradenigo, A. Sarracino, D. Villamaina, A. Vulpiani, J. Stat. Mech. L06001 (2012).